Effect of Gate-Field Dependent Mobility Degradation on Distortion Analysis in MOSFET's

Ronald van Langevelde, *Student Member, IEEE*, and François M. Klaassen

***Abstract*—Compact MOSFET models in contemporary circuit simulators fail to accurately describe distortion effects. In the ohmic region of the MOSFET, this failure is mainly due to inaccurate modeling of the gate-field dependent mobility degradation effect. In this paper a new model for mobility degradation is introduced which gives a major improvement in distortion analysis in the linear region for both n-type and p-type MOS transistors. Incorporating a gate voltage dependent series resistance, this model even gives good results for very short channel length devices.**

I. Introduction

In recent years, with the rise of Mixed Analog-Digital circuit design, the use of MOS transistors has not only been restricted to digital circuit design, but it has been extended to analog circuit design as well. The latter calls for more accurate compact MOSFET models which, apart from an accurate description of current-voltage characteristics, also give a good description of transconductance g_m $(= \frac{\partial I_D}{\partial V_{\mathrm{GS}}})$ and conductance g_d $(= \frac{\partial I_D}{\partial V_{\mathrm{DS}}})$ as a function of the terminal voltages. Nowadays, compact MOS models suitable for analog circuit design, such as the UCB BSIM3v3 and the Philips MOS9 model, have become available, nevertheless all models fail to predict distortion effects satisfactorily.

In MOS-circuits, due to the nonlinearity of MOS devices, a purely sinusoidal input signal results in an output signal that is not purely sinusoidal but has higher-order harmonics [1]; see Fig. 1. These higher-order harmonics are mainly induced by the higher-order derivatives of the current-voltage characteristics of the MOS transistor. For low-distortion applications the magnitude of the higher-order harmonics has to be minimized, using balanced circuit configurations even-order harmonics are canceled out [2] and in this case the third-order harmonic becomes the most influential one. For distortion applications the compact MOS model should therefore at least give an accurate description of $\frac{\partial^3 I_D}{\partial V_{\mathrm{GS}}{}^3}$, $\frac{\partial^3 I_D}{\partial V_{\mathrm{DS}}{}^3}$, and $\frac{\partial^3 I_D}{\partial V_{\mathrm{SB}}{}^3}$. This is not the case in contemporary MOS models [1].

This failure amongst others can be ascribed to the inaccurate, nonphysical modeling of physical phenomena such as mobility degradation, channel length modulation and velocity saturation. An improved circuit-level model can be achieved by implementing a more correct description of these phenomena in existing MOSFET models.

This paper concentrates on the effect of gate-field dependent mobility degradation in MOSFET's, in other words the dependence of the carrier mobility in the inversion layer on the transverse (gate) field. As MOS transistors biased in the weak or moderate-inversion region exhibit an exponential dependence on gate and drain voltage, these regions are not very suitable for low-distortion applications. Therefore this paper will focus on the strong-inversion region.

II. Theory of Mobility Degradation

The inversion layer mobility in Si MOSFET's is a very important physical quantity as a parameter to describe the drain current, and has therefore been subject to extensive research. It was found that the inversion layer mobility follows a universal curve independent of the substrate bias, the substrate impurity concentration or the gate oxide thickness when plotted as a function of the effective normal electric field E_{eff}, defined by [3]–[8]

$$E_{\mathrm{eff}} = \frac{(Q_{\mathrm{dep}} + \eta Q_{\mathrm{inv}})}{\epsilon_{Si}} \tag{1}$$

where Q_{dep} and Q_{inv} are the depletion and inversion layer charges per unit surface area, respectively. In most papers for an inversion layer on a (1 0 0) surface, η is taken to be 1/2 for electrons and 1/3 for holes. Generally, however, η is dependent on device process technology (e.g., doping profile, threshold voltage implant) [3], temperature [5], and surface orientation [8].

In most state-of-the-art MOSFET models a semi-empirical formulation is used to describe the dependence of surface mobility on effective normal field, based on classical surface diffuse scattering

$$\mu = \frac{\mu_0}{1 + \theta E_{\mathrm{eff}}} \tag{2}$$

where θ is an empirical parameter. With the scaling down of MOS transistors toward the requisite submicron dimensions, which involves the use of thinner gate oxide and higher substrate doping, the above formulation of channel mobility becomes more and more inaccurate. A more physical formulation should be used.

The thickness of the inversion layer is in the order of a few Å, which is smaller than the De Broglie wavelength of the carriers [9]; therefore, channel mobility has to be treated quantum-mechanically [6], [10], [11]. Quantum-mechanical

Manuscript received January 13, 1997; revised April 7, 1997. The review of this paper was arranged by Editor J. M. Vasi. This work was supported by the Dutch Technology Foundation (STW).

The authors are with the Electronic Devices Group, Faculty of Electrical Engineering, Eindhoven University of Technology, Eindhoven, The Netherlands.

Publisher Item Identifier S 0018-9383(97)07747-2.

0018–9383/97$10.00 © 1997 IEEE

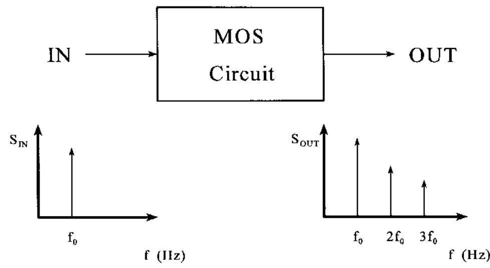

Fig. 1. Non-linearity of a MOS-circuit induces higher-order harmonics in the output signal $S_{\rm OUT}$ when a purely sinusoidal signal $S_{\rm IN}$ is applied to the input, this is called Harmonic Distortion.

self-consistent calculations show that energy subbands of electrons and holes are formed in the different energy valleys. The spacing of these subbands increases with increasing normal electric field. In other words in the weak inversion region where many electric subbands are occupied, quantum effects get washed out, on the other hand in the strong inversion region where very few electric subbands are occupied, quantum effects become important.

Actual modeling of scattering processes in the inversion layer is very complex due to the quantum-mechanical nature of these processes and the fact that in most cases more than one subband is filled. Therefore for mobility, a simplified semi-empirical approach was adopted. As has been done elsewhere [5], [12]–[16], mobility can be described by considering three mechanisms which dominate the scattering of charge carriers in the inversion layer at the Si-SiO$_2$-interface.

A. Coulomb Scattering (μ_C)

Charged centers near the Si-SiO$_2$ interface can be of the same charge type as the mobile inversion charge leading to Coulomb repulsion. This results in scattering, which is important for lightly inverted surfaces, high surface-charge densities or substrate doping concentrations, and less important for heavily inverted surfaces because of carrier screening. Coulomb scattering is not governed by a universal relation on $E_{\rm eff}$, therefore at low $Q_{\rm inv}$-values the universality law doesn't hold. This type of scattering is only of influence in the weak-inversion and moderate-inversion region and can therefore be neglected for the purpose of this work.

B. Phonon Scattering ($\mu_{\rm ph}$)

Surface phonons (surfons) from the quantum vibrations of the crystal lattice scatter the mobile charge carriers. Under the assumption that carriers in the inversion layer only occupy the lowest subband, the mobility determined by acoustic phonon scattering is described by [6], [8]

$$\mu_{\rm ph} \propto \left(\frac{11}{32}\cdot Q_{\rm inv} + Q_{\rm dep}\right)^{-\frac{1}{3}}. \tag{3}$$

Experimentally, it was found for both holes and electrons that

$$\mu_{\rm ph} \propto {E_{\rm eff}}^{-\frac{1}{3}}. \tag{4}$$

For electrons where $\eta = 1/2$, (4) deviates slightly from (3), which is ascribed to the fact that electrons occupy several subbands at intermediate values of effective field [6]. The assumption of single subband occupation in this case does not hold. The lowest hole subband compared to the lowest electron subband quickly reaches a high occupancy at lower field strength.

C. Surface Roughness Scattering ($\mu_{\rm sr}$)

The interface between the crystal silicon and the gate oxide is not atomically smooth. The above interface roughness scatters the mobile charge carriers. This type of scattering is especially important under strong inversion conditions because the strength of the interaction is governed by the distance of the carriers from the surface; the closer the carriers are to the surface, the stronger the scattering due to surface roughness will be. Under the assumption of single subband occupation and a Gaussian type autocorrelation function of interface roughness, $\mu_{\rm sr}$ can be described by [8]

$$\frac{1}{\mu_{\rm sr}} \propto {E_{\rm av}}^2 \cdot \int_0^\pi d\theta(1-\cos\theta)\exp\left(-\frac{1}{2}k^2{L_c}^2(1-\cos\theta)\right) \tag{5}$$

where L_c is the correlation length of interface roughness, k is the carrier wavelength, and $E_{\rm av}$ is the normal field averaged over the inversion layer. If we consider $E_{\rm av}$ as $E_{\rm eff}$, the value of η is to be 1/2 for a uniform doping profile. Non-uniform doping profiles will lead to different values of η [3].

In the limit that the correlation length is much smaller than the carrier wavelength ($L_c \ll k$), the mobility limited by surface roughness scattering $\mu_{\rm sr}$ reduces to

$$\mu_{\rm sr} \propto {E_{\rm eff}}^{-2} \tag{6}$$

The above dependence of surface roughness scattering corresponds to the experimentally found dependence of electron mobility on effective field.

For larger values of correlation length L_c, $\mu_{\rm sr}$ deviates from the dependence of ${E_{\rm eff}}^{-2}$ owing to the fact that the integral term in (5) depends on $Q_{\rm inv}$. For holes, it was found experimentally

$$\mu_{\rm sr} \propto {E_{\rm eff}}^{-1}. \tag{7}$$

The difference between (6) and (7) for electrons and holes is often ascribed to the fact that at high transverse fields holes tend to congregate further away from the interface than electrons do. The larger average distance leads to a reduced influence of the interface roughness and thus to less surface roughness scattering for holes.

The above-described mechanisms can be incorporated into one channel mobility (μ), using Matthiessen's rule

$$\frac{1}{\mu} = \frac{1}{\mu_B} + \frac{1}{\mu_{\rm sr}} + \frac{1}{\mu_{\rm ph}} \tag{8}$$

where μ_B is the carrier mobility limited by ionized impurity scattering and accoustic phonon scattering in the bulk material. Equation (8) leads to

$$\mu = \frac{\mu_B}{1+\theta_{\rm ph}{E_{\rm eff}}^{\frac{1}{3}} + \theta_{\rm sr}{E_{\rm eff}}^{n}} \tag{9}$$

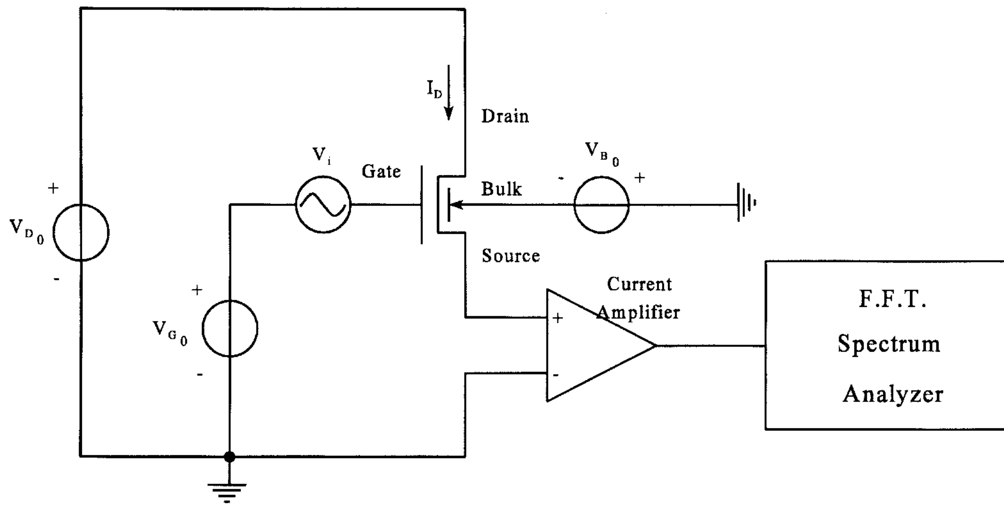

Fig. 2 Measurement setup for distortion behavior of single MOS transistor.

where θ_{ph} and θ_{sr} are empirical parameters, and $n = 2$ for electrons and $n = 1$ for holes.

Strictly speaking Matthiessen's rule is not valid because it tacitly assumes that the momentum relaxation times due to the different scattering mechanisms have the same energy dependence. In order to correctly account for the various scattering sources, a weighted statistical averaging of the relaxation times should be performed. Nevertheless Matthiessen's rule should give a good first-order approximation, especially when valley repopulation is taken into account [6].

III. Implementation in a Circuit-Level Model

As we are interested in the effect of mobility degradation on the distortion behavior of MOSFET's, the mobility model (9) has to be implemented in the drain current equation. For this purpose we only concentrate on the ohmic region at low drain-source voltages, so that the effect of longitudinal electric field can be neglected. For sufficiently small V_{DS}, the carrier mobility is assumed to be constant along the channel. Now in strong-inversion, the drain current I_D in zero-order approximation can be expressed as [17]

$$I_D = \mu C_{\mathrm{OX}} \frac{W}{L}\left(V_{\mathrm{GS}} - V_{\mathrm{th}} - \frac{1}{2}V_{\mathrm{DS}}\right)V_{\mathrm{DS}} \qquad (10)$$

where C_{OX} is the oxide capacitance per unit area, W and L are the effective channel width and length, respectively, and V_{th} is the threshold voltage dependent on bulk bias V_{SB}. For the mobility μ (9) has to be used with $n = 2$ or $n = 1$ in the case of n-type or p-type MOS transistors, respectively.

The effective normal field E_{eff} is expressed in terms of Q_{inv} and Q_{dep} [3]

$$Q_{\mathrm{inv}} = C_{\mathrm{OX}}(V_{\mathrm{GS}} - V_{\mathrm{th}}) \qquad (11)$$

$$Q_{\mathrm{dep}} = C_{\mathrm{OX}}(V_{\mathrm{th}} - V_{\mathrm{FB}} - \phi_s) \qquad (12)$$

where V_{FB} is the flat-band voltage and ϕ_s is the surface potential which may be approximated by twice the Fermi potential ϕ_F.

The drain current equation (10) should give a good description of the actual current and its higher-order derivatives for long-channel transistors. However with decreasing channel length, series resistance effects become important and these effects have to be incorporated. Series resistance can be implemented in the drain current equation as follows (see Appendix I):

$$I_D \approx \frac{\mu \cdot C_{\mathrm{OX}} \cdot \frac{W}{L} \cdot \left(V_{\mathrm{GS}} - V_{\mathrm{th}} - \frac{1}{2} \cdot V_{\mathrm{DS}}\right) \cdot V_{\mathrm{DS}}}{1 + 2 \cdot \mu \cdot C_{\mathrm{OX}} \cdot \frac{W}{L} \cdot R_S \cdot \left(V_{\mathrm{GS}} - V_{\mathrm{th}} - \frac{1}{2} \cdot V_{\mathrm{DS}}\right)} \qquad (13)$$

where R_S is the series resistance.

The series resistance in the drain/source region of a MOS transistor consists of four components: 1) a contact resistance, 2) a sheet resistance, 3) a spreading resistance due to current crowding in the vicinity of the channel end, and 4) an accumulation layer resistance. The latter is due to overlap of the gate polysilicon on the drain/source region, and is gate voltage dependent. For correct modeling the gate voltage dependency of the series resistance has to be implemented [18]

$$R_S = a_0 + \frac{a_1}{a_2 + (V_{\mathrm{GS}} - V_{\mathrm{th}})} \qquad (14)$$

where a_0, a_1, and a_2 are empirical parameters.

IV. Measurement Results and Discussion

The distortion behavior of a single transistor is determined by the higher-order derivatives of the drain current I_D with respect to any terminal voltage [1]. As the mobility degradation is dependent on the normal electric field, we are particularly interested in $\frac{\partial I_D}{\partial V_{\mathrm{GS}}}$, $\frac{\partial^2 I_D}{\partial V_{\mathrm{GS}}^2}$, and $\frac{\partial^3 I_D}{\partial V_{\mathrm{GS}}^3}$ at low V_{DS} where the influence of longitudinal electric field can be neglected. These higher-order derivatives can be determined by applying a purely sinusoidal signal to the gate terminal and by measuring the higher-order harmonics in the drain current I_D using a signal analyzer, see Fig. 2. The frequency of the sinusoidal signal is 1 kHz, so that the influence of capacitances can be neglected. If the amplitude of the sinusoidal signal is not chosen too large, the amplitude of the higher-order harmonics corresponds to the higher-order derivatives (see Appendix II). This procedure can be repeated for different bias conditions (V_{G0} and V_{B0}).

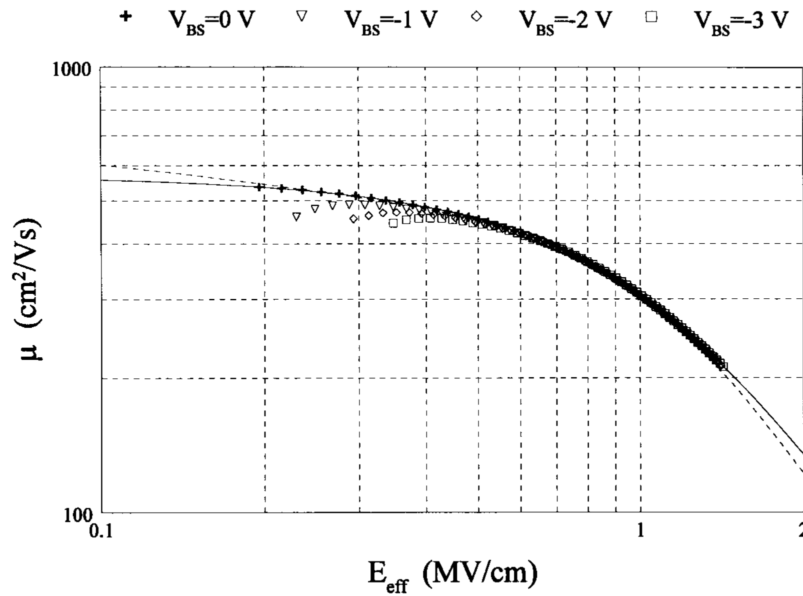

Fig. 3 Measured electron mobility μ as a function of effective field $E_{\rm eff}$ ($\eta = 0.68$) for an n-type MOS transistor with $W = 20$ μm and $L = 20$ μm for different bulk voltages V_{BS}. Results of mobility model (9) with $n = 2$ (solid line) and (15) (dotted line) are also shown.

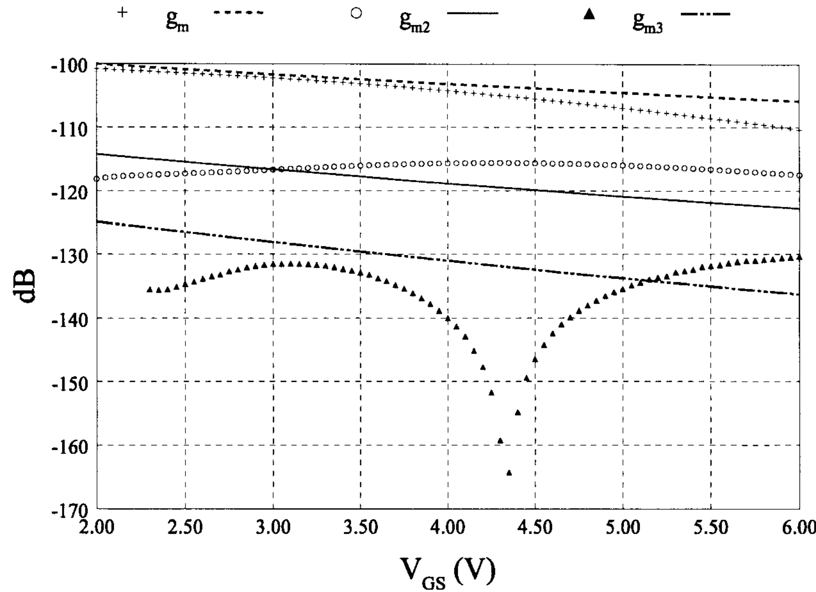

Fig. 4. Measured (symbols) and modeled (lines) values of $\frac{\partial I_D}{\partial V_{\rm GS}}$ (g_m), $\frac{\partial^2 I_D}{\partial V_{\rm GS}{}^2}$ (g_{m2}), and $\frac{\partial^3 I_D}{\partial V_{\rm GS}{}^3}$ (g_{m3}) as a function of gate voltage $V_{\rm GS}$ for an n-type MOS transistor with $W = 10$ μm, $L = 10$ μm at $V_{\rm SB} = 0$ V, using (2) and (10).

Measurements were performed on both n-type and p-type MOSFET's from a commercial submicron process with a channel width W of 10 μm and different values of channel length L. The minimum channel length is 0.8 μm. The n-channel MOSFET's make use of an LDD-structure, and the p-channel MOSFET's are of the buried type. The gate oxide thickness is about 150 Å, and the zero bias threshold voltage $V_{\rm th0}$ is 0.9 V and -1.1V for n-type and p-type transistors, respectively.

A. NMOS-Devices

Using the split C-V method as described in [19], mobility measurements were performed on n-type MOS transistors, see Fig. 3. Universality of μ with effective field $E_{\rm eff}$ was found for $\eta = 0.68$, which differs from the expected value of 0.5. This is probably caused by the nonuniform substrate concentration due to the threshold voltage implantation [3].

In Fig. 4, the measured values of $\frac{\partial I_D}{\partial V_{\rm GS}}, \frac{\partial^2 I_D}{\partial V_{\rm GS}{}^2}$, and $\frac{\partial^3 I_D}{\partial V_{\rm GS}{}^3}$ for a long-channel n-type MOS transistor ($L = 10$ μm) in the linear region ($V_{D0} = 0.1$ V) are given as a function of $V_{\rm GS}$. For this case series resistance effects are negligible, and thus the derivatives are mainly determined by mobility degradation. The commonly used (2) was optimized using the measurement results, and the modeled results are also shown in Fig. 4. As can be seen the zero-crossing in the third-order derivative is not predicted by (2). Clearly, the simulations and

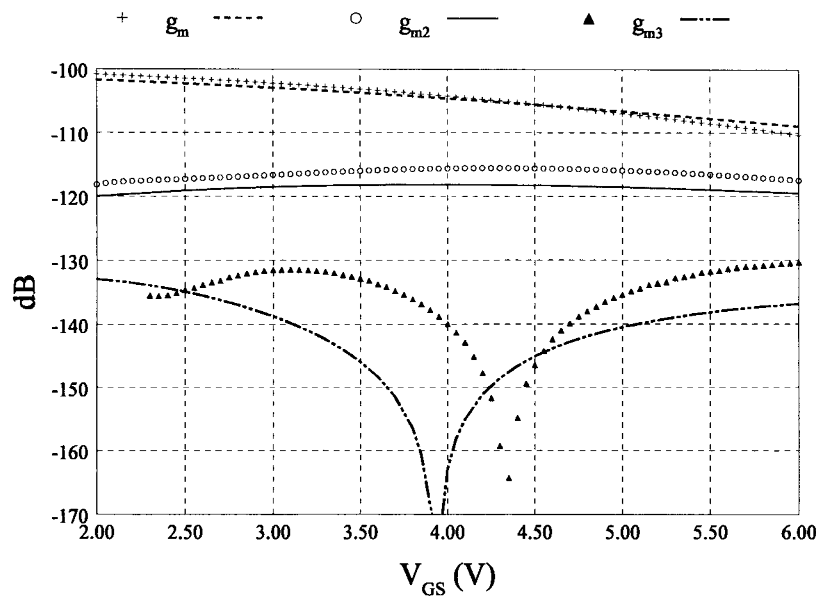

Fig. 5. Same as Fig. 3, using (9) and (10) with $n = 2$.

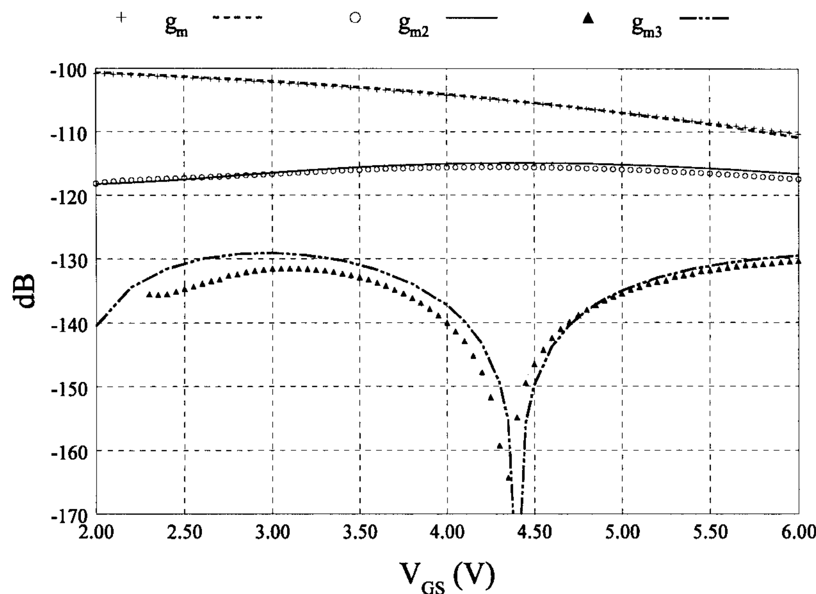

Fig. 6. Same as Fig. 3, using (15) and (10).

measurements do not agree and therefore a better description of surface mobility has to be used.

Next, (9) with $n = 2$ was optimized, and the resulting μ-E_{eff}-curve can be seen in Fig. 3 (solid line). Equation (9) gives an accurate description of mobility μ for a large range of E_{eff}-values. The modeled distortion analysis results are given in Fig. 5. Equation (9) results in a substantial improvement with regard to (2); it predicts a zero-crossing in the third-order derivative, nevertheless the third-order derivative is still not modeled well.

Closer examination of the distortion measurement results shows that phonon scattering dominates at low values of V_{GS} and surface roughness scattering dominates at high values of V_{GS}, however the incorporation of these scattering mechanisms into one mobility equation using Matthiessen's rule doesn't give accurate results. Matthiessen's rule is only valid for energy independent processes. At intermediate values of E_{eff} electrons tend to populate different energy subbands in both the longitudinal and the transverse energy valleys, so for this case Matthiessen's rule is not really valid. This result was also found in [6] for electrons on a (1 0 0) surface, where the authors suggested that this effect is due to valley repopulation. In other words, the electrons tend to populate in the transverse energy valleys as the gate field increases. To account for the nonvalidity of Matthiessen's rule, a different sharper transition from phonon scattering to surface roughness scattering was opted for

$$\mu = \frac{\mu_B}{1 + \sqrt{\theta_{\text{ph}} E_{\text{eff}}^{\frac{2}{3}} + \theta_{\text{sr}} E_{\text{eff}}^{4}}}. \tag{15}$$

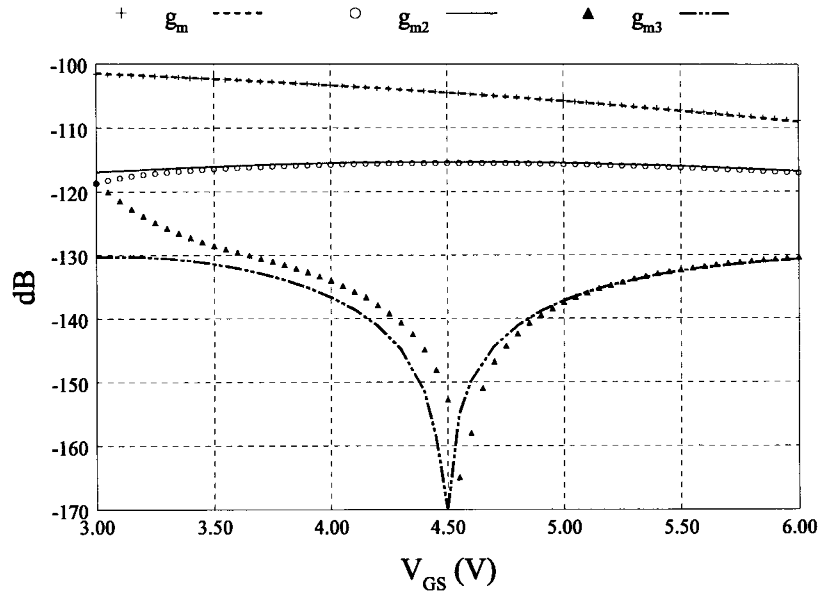

Fig. 7. Measured (symbols) and modeled (lines) values of $\frac{\partial I_D}{\partial V_{\mathrm{GS}}}$ $\{g_m\}$, $\frac{\partial^2 I_D}{\partial V_{\mathrm{GS}}{}^2}$ $\{g_{m2}\}$ and $\frac{\partial^3 I_D}{\partial V_{\mathrm{GS}}{}^3}$ $\{g_{m3}\}$ as a function of gate voltage V_{GS} for an n-type MOS transistor with $W = 10$ μm, $L = 10$ μm at $V_{\mathrm{SB}} = 5$ V, using (15) and (10).

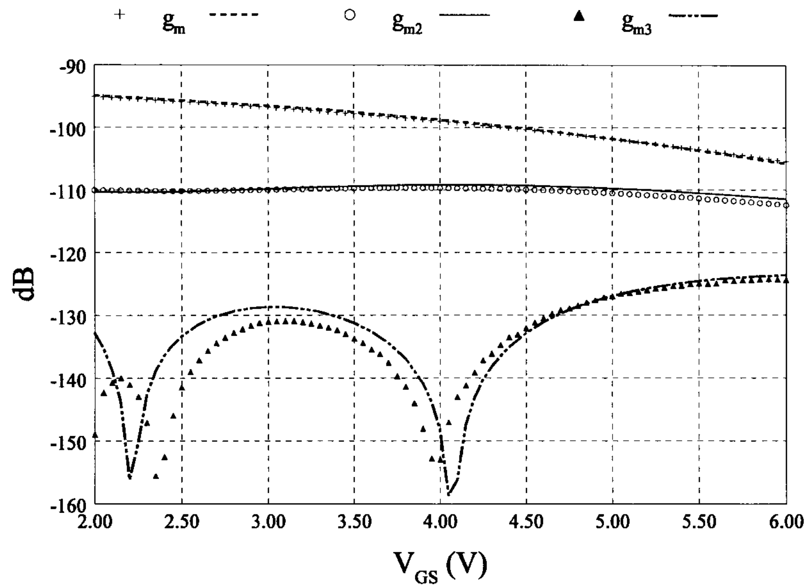

Fig. 8. Measured (symbols) and modeled (lines) values of $\frac{\partial I_D}{\partial V_{\mathrm{GS}}}$ $\{g_m\}$, $\frac{\partial^2 I_D}{\partial V_{\mathrm{GS}}{}^2}$ $\{g_{m2}\}$, and $\frac{\partial^3 I_D}{\partial V_{\mathrm{GS}}{}^3}$ $\{g_{m3}\}$ as a function of gate voltage V_{GS} for an n-type MOS transistor with $W = 10$ μm, $L = 5$ μm at $V_{\mathrm{SB}} = 0$ V, using (15) and (13).

At low and high values of the effective normal field E_{eff}, $1/\mu$ reduces to the $E_{\mathrm{eff}}{}^{\frac{1}{3}}$ and the $E_{\mathrm{eff}}{}^2$ dependence in both (9) and (15). Equation (15) was optimized, and the resulting μ-E_{eff}-curve can be seen in Fig. 3 (dotted line). As can be seen, (15) gives results as accurate as (9) for the range of E_{eff}-values under examination. The modeled distortion analysis results for (15) are given in Fig. 6. As can be seen the sharper transition from phonon scattering limited mobility to surface roughness scattering limited mobility in (15) leads to a more accurate description of the higher-order derivatives. Even the zero-crossing in the third-order derivative is predicted accurately.

The measurements have been repeated for different values of bulk voltage V_{SB}. The measurement results and the simulation results of (15) for $V_{\mathrm{SB}} = 5$ V are given in Fig. 7. Once again, (15) gives good results. Only for small values of V_{GS}, the simulation results for $\frac{\partial^3 I_D}{\partial V_{\mathrm{GS}}{}^3}$ deviate from the measurement results. This is due to the effect of Coulomb scattering which becomes more important with increasing bulk bias V_{SB} as can be seen in Fig. 3.

The effect of series resistance can be seen in Fig. 8 and 9 where the measurement results and simulation results using (13), (14), and (15) are given for $L = 5$ μm and 0.8 μm, respectively. The distortion behavior changes drastically with decreasing channel length L. For $L = 5$ μm two zero-crossings

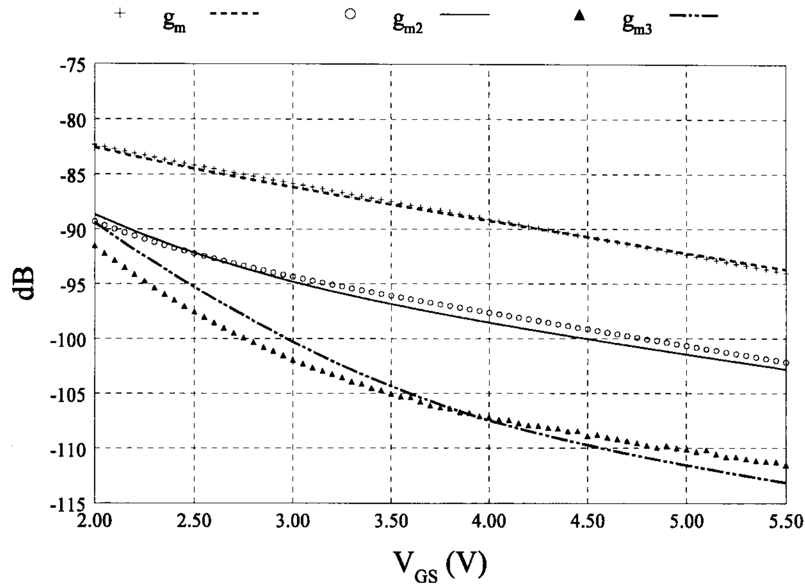

Fig. 9. Same as Fig. 8, for $L = 0.8$ μm.

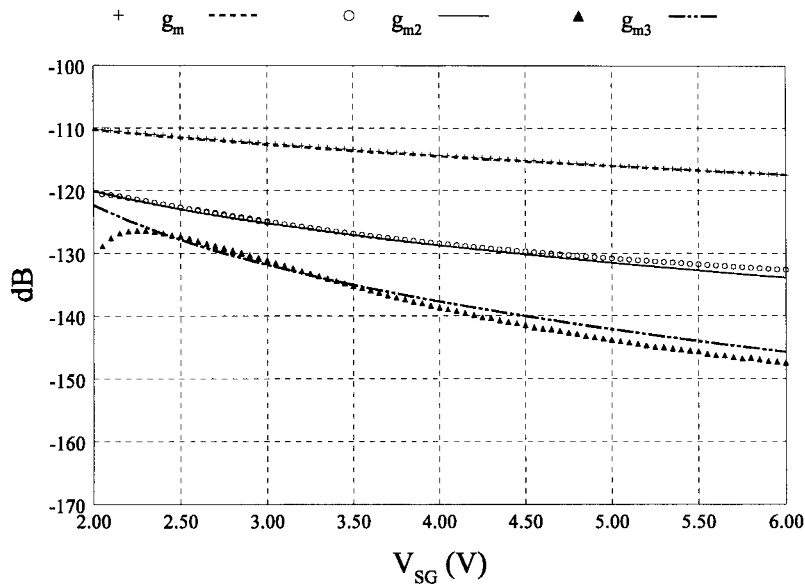

Fig. 10. Measured (symbols) and modeled (lines) values of $\frac{\partial I_D}{\partial V_{\rm GS}}$ $\{g_m\}$, $\frac{\partial^2 I_D}{\partial V_{\rm GS}^2}$ $\{g_{m2}\}$, and $\frac{\partial^3 I_D}{\partial V_{\rm GS}^3}$ $\{g_{m3}\}$ as a function of gate voltage $V_{\rm GS}$ for a p-type MOS transistor with $W = 10$ μm, $L = 10$ μ m at $V_{\rm SB} = 0$ V, using (9) and (10) with $n = 1$.

can be seen in the third-order derivative, at low values of gate voltage the effect of series resistance introduces a new zero-crossing, whereas at high values of gate voltage the ${E_{\rm eff}}^2$ term is still dominant and the third-order derivative behaves the same as for long-channel transistors. For $L = 0.8$ μm no more zero-crossings can be seen in the third-order derivative, as the effect of series resistance is dominant for all values of gate voltage. Equations (13)–(15) give an accurate description of distortion behavior for all channel lengths. The incorporation of the gate voltage dependency of series resistance is important for channel lengths smaller than 2 μm.

B. PMOS-Devices

A value for η of 1/3 was found to give accurate results for holes, which corresponds to theory. In Fig. 10, the measured values of $\frac{\partial I_D}{\partial V_{\rm GS}}, \frac{\partial^2 I_D}{\partial V_{\rm GS}^2}$, and $\frac{\partial^3 I_D}{\partial V_{\rm GS}^3}$ for a long-channel p-type MOS transistor ($L = 10$ μm) in the ohmic region ($V_{D0} = -0.1$ V) are given as a function of $V_{\rm GS}$. Clearly, the hole mobility degradation is completely different from the electron mobility degradation, which can be ascribed to the difference in surface roughness scattering. Equation (9) with $n = 1$ was optimized using the measurement results. The simulation results are also given in Fig. 10, they correspond well to the measurement results. Apparently for holes Matthiessen's rule is valid; this might be due to the fact that holes tend to populate in the

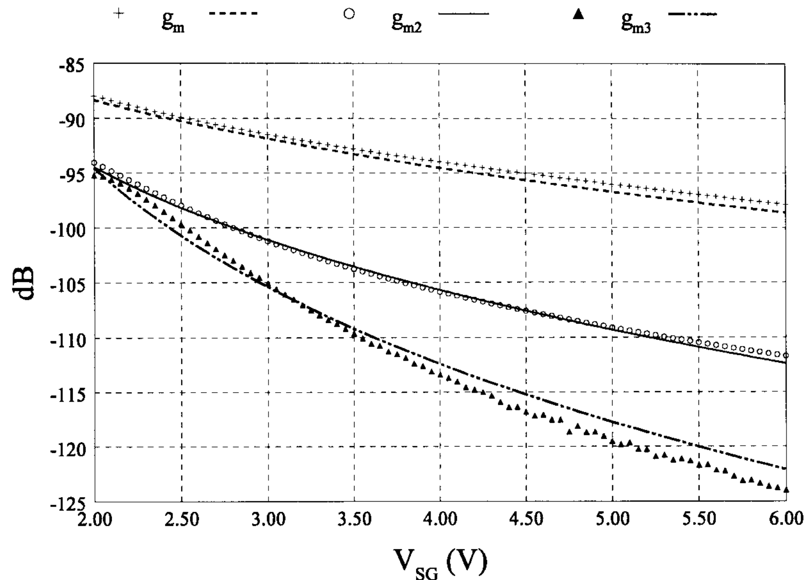

Fig. 11. Measured (symbols) and modeled (lines) values of $\frac{\partial I_D}{\partial V_{\rm GS}}$ $\{g_m\}$, $\frac{\partial^2 I_D}{\partial V_{\rm GS}{}^2}$ $\{g_{m2}\}$, and $\frac{\partial^3 I_D}{\partial V_{\rm GS}{}^3}$ $\{g_{m3}\}$ as a function of gate voltage $V_{\rm GS}$ for a p-type MOS transistor with $W = 10$ μm, $L = 0.8$ μm at $V_{\rm SB} = 0$V, using (9) and (13) with $n = 1$.

lowest energy subband even at lower field strengths [6], [9].

The influence of series resistance can be observed in Fig. 11 where the measurement results and simulation results using (9), (13), and (14) are given for $L = 0.8$ μm. As the dependence on gate voltage $V_{\rm GS}$ for surface roughness scattering ($\propto E_{\rm eff}$) is basically the same as for the series resistance effect ($\propto V_{\rm GS} - V_{\rm th}$), the distortion behavior for p-type MOSFET's does not change very much with decreasing channel length L. Equations (9), (13), and (14) give an accurate description of distortion behavior for all values of channel length.

V. Conclusions

An accurate, physical description of mobility degradation in circuit-level MOSFET models is essential for distortion analysis. The difference in quantum-mechanical behavior of electrons and holes in the inversion layer leads to different models for electron and hole mobility. Although in strong-inversion both hole and electron mobility are mainly limited by the same two scattering mechanisms, i.e., phonon scattering and surface roughness scattering, they still exhibit a different dependence on effective normal field $E_{\rm eff}$. New mobility models for electrons and holes have been found, which can be incorporated in compact MOSFET models. For long-channel MOS transistors at low drain voltage $V_{\rm DS}$, these improved MOS models describe the drain current I_D and its higher-order derivatives $\frac{\partial I_D}{\partial V_{\rm GS}}, \frac{\partial^2 I_D}{\partial V_{\rm GS}{}^2}$ and $\frac{\partial^3 I_D}{\partial V_{\rm GS}{}^3}$ accurately for a large region of gate voltages and bulk voltages. The accurate results of these MOS models can be extended to short channel length transistors, when the gate voltage dependency of series resistance is also incorporated in the models.

In order to minimize distortion in circuits, it is often important to make the third-order derivative zero. As can be seen from Figs. 4 through 8, this is only possible for long-channel n-type MOS transistors, where mobility degradation is more dominant than the effect of series resistance. The DC-biasing point for which $\frac{\partial^3 I_D}{\partial V_{\rm GS}{}^3}$ becomes zero, is essentially determined by the presence of the $E_{\rm eff}{}^2$ term and can be accurately predicted using (15). P-type MOS transistors are less suitable for distortion applications where mobility degradation is the limiting factor.

Appendix I

From a viewpoint of circuit simulation time it is desirable to include the series resistance directly into the MOSFET model without adding additional nodes. In the linear region the drain current expression for a MOS transistor without series resistance is given by (10). In the presence of source and drain resistance, R_S and R_D, the internal bias values $V_{\rm GS}$, $V_{\rm DS}$, and $V_{\rm SB}$ are lowered and have to be replaced by

$$\begin{aligned} V_{\rm GS} &\rightarrow V_{\rm GS} - I_D \cdot R_S \\ V_{\rm DS} &\rightarrow V_{\rm DS} - I_D \cdot (R_S + R_D) \\ V_{\rm SB} &\rightarrow V_{\rm SB} + I_D \cdot R_S. \end{aligned}$$

Neglecting the effect of series resistance on the effective normal field $E_{\rm eff}$ and on threshold voltage $V_{\rm th}$, the drain current can be expressed as

$$I_D \approx \frac{\frac{2\beta\left(V_{\rm GS}-V_{\rm th}-\frac{1}{2}V_{\rm DS}\right)V_{\rm DS}}{1+\beta(R_S+R_D)(V_{\rm GS}-V_{\rm th})-\beta R_D V_{\rm DS}}}{1+\sqrt{1-\frac{2\beta^2(R_S{}^2-R_D{}^2)\left(V_{\rm GS}-V_{\rm th}-\frac{1}{2}V_{\rm DS}\right)V_{\rm DS}}{(1+\beta(R_S+R_D)(V_{\rm GS}-V_{\rm th})-\beta R_D V_{\rm DS})^2}}} \tag{16}$$

where β is given by

$$\beta = \mu C_{\rm OX}\frac{W}{L}. \tag{17}$$

For small values of $V_{\rm DS}$ the drain resistance R_D is equal to the source resistance R_S [18], and (16) reduces to (13).

Appendix II

In the measurement set-up in Fig. 2, the drain current I_D can be expanded in a Taylor series

$$I_D = b_0 + b_1 \cdot v_i + b_2 \cdot {v_i}^2 + b_3 \cdot {v_i}^3 + \ldots = \sum_{i=0}^{\infty} b_i \cdot {v_i}^i \quad (18)$$

where v_i is a purely sinusoidal signal

$$v_i = V_P \cdot \sin(\omega t) \quad (19)$$

and

$$b_i = \frac{1}{i!} \cdot \frac{\partial^i I_D}{\partial {V_{\mathrm{GS}}}^i}\bigg|_{V_{D0}, V_{G0}, V_{B0}}. \quad (20)$$

The drain current (18) can be rewritten in terms of $sin(n\omega t)$

$$I_D = c_0 + c_1 \cdot \sin(\omega t) + c_2 \cdot \cos(2\omega t) + c_3 \cdot \sin(3\omega t) + \ldots \quad (21)$$

The components c_1, c_2 and c_3 are measured by the spectrum analyzer, and can be written as

$$c_1 = b_1 \cdot V_P + \frac{3}{4} \cdot b_3 \cdot {V_P}^3 + \frac{5}{8} \cdot b_5 \cdot {V_P}^5 + \ldots \quad (22)$$

$$c_2 = -\frac{1}{2} \cdot b_2 \cdot {V_P}^2 - \frac{1}{2} \cdot b_4 \cdot {V_P}^4 - \ldots \quad (23)$$

$$c_3 = -\frac{1}{4} \cdot b_3 \cdot {V_P}^3 - \frac{5}{16} \cdot b_5 \cdot {V_P}^5 - \ldots \quad (24)$$

When a small enough value is chosen for the amplitude V_P, (22)–(24) reduce to

$$c_1 \approx b_1 \cdot V_P \quad (25)$$

$$c_2 \approx -\frac{1}{2} \cdot b_2 \cdot {V_P}^2 \quad (26)$$

$$c_3 \approx -\frac{1}{4} \cdot b_3 \cdot {V_P}^3. \quad (27)$$

In this way, the higher-order derivatives $\frac{\partial I_D}{\partial V_{\mathrm{GS}}}$, $\frac{\partial^2 I_D}{\partial {V_{\mathrm{GS}}}^2}$, and $\frac{\partial^3 I_D}{\partial {V_{\mathrm{GS}}}^3}$ can be calculated in a straight-forward manner from the measured harmonics.

Acknowledgment

The authors wish to thank D. B. M. Klaassen and R. D. M. Velghe of Philips Research Laboratories, Eindhoven, The Netherlands, for supplying the devices.

References

[1] G. Groenewold and W. J. Lubbers, "Systematic distortion analysis for MOSFET integrators with use new MOSFET model," *IEEE Trans. Circuits Syst.*, vol. CAS-41, pp. 569–580, Sept. 1994.

[2] G. Wilson and P. K. Chan, "Analysis of nonlinearities in MOS floating resistor networks," *IEE Proc. Circuits Devices Syst.*, vol. 141, no. 2, pp. 82-88, 1994.

[3] T. J. Krutsick and M. H. White, "Consideration of doping profiles in MOSFET mobility modeling," *IEEE Trans. Electron Devices*, vol. ED, pp. 1153–1155, July 1988.

[4] S. Takagi, M. Iwase, and A. Toriumi, "On the universality of inversion-layer mobility in N- and P-channel MOSFET's," in *IEDM Tech. Dig.*, 1988, pp. 398–401.

[5] C. -L. Huang and G. S. Gildenblat, "Measurements and modeling of the n-channel MOSFET inversion layer mobility and device characteristics in the temperature range 60–300 K," *IEEE Trans. Electron Devices*, vol. 37, pp. 1289–1300, May 1990.

[6] K. Lee, J.-S. Choi, S.-P. Sim, and C.-K. Kim, "Physical understanding of low-field carrier mobility in silicon MOSFET inversion layer," *IEEE Trans. Electron Devices*, vol. 38, pp. 1905-1911, Aug. 1991.

[7] S. Takagi, A. Toriumi, M. Iwase, and H. Tango, "On the universality of inversion layer mobility in Si MOSFET's: Part I—Effects of substrate impurity concentration," *IEEE Trans. Electron Devices*, vol. 41, pp. 2357–2362, Feb. 1994.

[8] ——, "On the universality of inversion Layer mobility in Si MOSFET's: Part II—Effects of surface orientation," *IEEE Trans. Electron Devices*, vol. 41, pp. 2363–2368, Feb. 1994.

[9] C. Moglestue, "Self-consistent calculation of electron and hole inversion charges at silicon-silicon dioxide interfaces," *J. Appl. Phys.*, vol. 59, no. 9, pp. 3175–3183, 1986.

[10] M. S. Lin, "The classical versus the quantum mechanical model of mobility degradation due to the gate field in MOSFET inversion layers," *IEEE Trans. Electron Devices*, vol. ED-32, pp. 700-710, Mar. 1985.

[11] ——, "A better understanding of the channel mobility of Si MOSFET's based on the physics of quantized subbands," *IEEE Trans. Electron Devices*, vol. 35, pp. 2406–2411, Dec. 1988.

[12] A. J. Walker and P. H. Woerlee, "A mobility model for MOSFET device simulation," *J. Phys. Coll.*, vol. C4, pp. 265–268, 1988.

[13] D. S. Jeon and D. E. Burk, "MOSFET electron inversion layer mobilities—A physically based semi-empirical model for a wide temperature range," *IEEE Trans. Electron Devices*, vol. 36, pp. 1456–1463, Aug. 1989.

[14] V. M. Agostinelli, H. Shin, and A. F. Tasch, "A comprehensive model for inversion layer hole mobility for simulation of submicrometer MOSFET's," *IEEE Trans. Electron Devices*, vol. 38, pp. 151–159, Jan. 1991.

[15] C.-L. Huang and N. D. Arora, "Characterization and modeling of the n- and p-channel MOSFET's inversion-layer mobility in the range 25–150 C," *Solid-State Electron.*, vol. 37, no. 1, pp. 97–103, 1994.

[16] K.-S. Min and K. Lee, "Temperature-dependent hole and electron mobility models for CMOS circuit simulation," *IEEE Trans. Electron Devices*, vol. 42, pp. 1956–1961, Nov. 1995.

[17] Y. P. Tsividis, *Operation and Modeling of the MOS Transistor*. New York: McGraw-Hill, 1987, pp. 123–130.

[18] J. A. M. Otten and F. M. Klaassen, "A novel technique to determine the gate and drain bias dependent series resistance in drain engineered MOSFET's using one single device," *IEEE Trans. Electron Devices*, vol. 43, pp. 1478–1488, Sept. 1996.

[19] C.-L. Huang, J. V. Faricelli, and N. D. Arora, "A new technique for measuring MOSFET inversion layer mobility," *IEEE Trans. Electron Devices*, vol. 40, pp. 1134–1139, June 1993.

Ronald van Langevelde (S'95) was born in Terneuzen, The Netherlands, on May 18, 1971. He received the Master's degree in electrical engineering (cum laude) from the Eindhoven University of Technology, The Netherlands, in 1994. He is currently pursuing the Ph.D. degree in electrical engineering at the Eindhoven University of Technology. His research involves MOSFET device physics, circuit-level MOSFET modeling, and distortion analysis in circuit-design.

François M. Klaassen was born in 1934. He received the M.Sc. and Ph.D. degrees in physics from the Free University of Amsterdam, The Netherlands, in 1959 and 1961, respectively.

From 1961 until 1993, he was at the Philips Research Laboratories of Eindhoven, The Netherlands. During this period, he was with the Research Laboratories of Northern Telecom, Ottawa, Ont., Canada, for several years. In 1982, he was appointed as Chief Scientist of Philips Research. Major subjects of his research activities have been, successively, photoconductive layers for video cameras, noise in various types of transistors, UHF MOSFET tetrodes, physical electronics of IC components (I^2L, BICMOS, MOSFET scaling, small-size devices of s-RAM), and circuit-level MOSFET modeling. Since 1971, he has been working as a part-time Professor in Microelectronics at the Eindhoven University of Technology and, after retiring from Philips, also at the RWTH of Aachen, Germany. He has been the promotor of 15 Ph.D. candidates and has been responsible for 60 M.Sc. theses. Among his numerous publications is a book coauthored with H. C. de Graaff entitled *Compact Transistor Modelling for Circuit Design* (Vienna: Springer-Verlag).

Dr. Klaassen has been serving, since 1980, as Regional Editor, and later as Editor, of *Solid-State Electronics.*